Thermochimica Acta, 155 (1989) 115–134
Elsevier Science Publishers B.V., Amsterdam – Printed in The Netherlands

ANALYSIS OF A MARTENSITIC TRANSFORMATION BY OPTICAL MICROSCOPY, ACOUSTIC EMISSION DETECTION, RESISTANCE MEASUREMENTS AND DIFFERENTIAL SCANNING CALORIMETRY

A. AMENGUAL and V. TORRA

Dep. Fisica, Universitat de les Illes Balears, E-07071 Palma de Mallorca (Spain)

A. ISALGUE and F. MARCO

Dep. Fisica Aplicada, Universitat Politecnica de Catalunya, E-08028 Barcelona (Spain)

(Received 28 March 1989)

ABSTRACT

A system has been developed which allows the control and programming of temperature within a working space in order to study hysteresis cycles in shape memory alloys. Temperature detection is by means of a Pt-100 resistance with a resolution of 0.001 ohm (0.003 K). Our experimental set-up, with a sample of 1 g in mass, can operate with a resolution and reproducibility of about 0.005 K. The maximum amplitude used is near 70 K. For intervals of 2 K, the minimum period lies around 200 s and for intervals of 50 K around 1500 s.

The Peltier effect is used for heating and cooling. It is excited by a current which provides a power supply controlled by a computer. The system has been built in a very simple way, working at around room temperature.

This controlled system has been applied to the study of the evolution of the martensitic transformation. With this goal, one needs to acquire one or more simultaneous measurements on a given specimen. The available measurements are as follows.

(a) Acoustic emission (A.E.) ring-down counting (MCS) or its classification by pulse high amplitude (PHA). In both cases a multichannel analyser is used.

(b) Optical microscopy observation (up to 700×) and simultaneous video recording for further study (260–360 K). The resolution of the optical microscope (1 μm) is such that the small dimensional changes occurring during the growth of the martensite plates can be observed. When coupled with A.E., this indicates the connection between the accelerating movements of the interface and the acoustic activity.

(c) Resistance changes. In this case, the use of techniques such as the lock-in method allows a resolution near 0.1% for resistance values of 1 mΩ to be obtained which is near the resolution available with calorimetry and acoustic emission. Therefore, it could be used in the study of the elementary transformation tipus burst.

(d) Unconventional DSC (223–353 K). With suitable signal processing, this has a resolution near 1 μV, equivalent to 3 μW, which can monitor the energetic changes associated with the thermal cycles when austenite and martensite coexist. In particular, the hysteresis cycles activated by global or partial temperature (Mf or Af not achieved) can be analysed.

INTRODUCTION

Most applications of shape memory alloys rely on a precise knowledge of the hysteresis cycle of the alloy. Of particular concern to us is the fact that the hysteresis cycle of a given alloy may depend on previous thermomechanical treatments [1–3] and, as a consequence, the properties of a given alloy may be substantially altered after repeated cycling through the transformation region. There are a number of factors that determine the hysteresis cycle of an alloy. Among them are the concentration of defects (vacancies, dislocations, etc.), the state of atomic order of the alloy and the existence of precipitates [4]. Their effect on the kinetics of the transformation and on the hysteresis cycle may be different after a sequence of forward and reverse transformations or cycles. It is in fact well-known that, in some cases, repeated cycling may lead to a loss of the double memory effect.

Most efforts to date have been aimed at a precise characterization of the macroscopic aspects of the hysteresis cycle of particular alloys, but little is known about the mechanisms that determine the cycle itself and how they are affected by the external fields used to induce the transformation [5]. Previous work in this direction seems to suggest that the motion of a single interface during the transformation of the thermoelastic alloy is not continuous but, rather, proceeds through a sequence of discontinuous motions which are accompanied by the release of elastic energy and latent heat. The mechanisms responsible for these elementary motions of the interface must come into play in the determination of the hysteresis cycle.

Recent experimental work has shown that the temperature resolution which is needed in order to isolate and characterize these elementary events is of the order of 0.01 K [10], one order of magnitude higher than the resolution of the devices which are being used to investigate the properties of martensitic transformations. In this paper we present the details of a new experimental set-up which attains the necessary resolution in temperature and allows the determination of resistances and acoustic and thermal energies released during the elementary motions of the interface. We have also been able to detect discontinuous changes in the resistance of the sample and to correlate them with sudden releases of acoustic and thermal energies and with discontinuous motions of a single interface. We expect that further study of the transformation at this level of resolution will provide new clues into the microscopic mechanisms which affect the kinetics of the transformation and, as a consequence, that ultimately determine the hysteresis cycle itself.

We have focused our attention on the determination of the acoustic and thermal energy released during the transformation and on the changes in the resistance of the sample. Recent work with differential scanning calorimetry (DSC) and acoustic emission detection (AED) on monocrystalline samples has shown that these two types of measurements can be used as sensitive tools to follow the dynamics of the transformation [6,7]. They have also provided some complementary information: the study of partial cycles, for example, suggests that what was originally thought to be a stochastic evolution of the material can be, in fact, traced to secondary effects related to poor control of the temperature [5,8,9]. (A partial cycle is defined as follows; the initial state of the system comprises a bulk region of parent phase and a bulk region of martensite. The external control parameters are then changed in such a way that a final state is reached in which the relative fraction of martensite is larger. The path is then reversed until the initial state is reached.) This work has also shown that the existence of intrinsic hysteresis [10,11], the existence of surface martensite [12] and temperature gradients inside the material can change the morphology of the transformation.

In order to simplify the interpretation of some results, we have also chosen to follow the motion of the interfaces bounding a single domain of martensite. Weak external stresses can be used such that the growth of a single variant is enhanced and a reproducible behaviour between successive cycles can be observed [13]. A necessary condition required to maintain such a degree of reproducibility is the very rigorous control of the temperature of the sample.

The development of theoretical models of the transformation [14] require reliable estimates of the energy changes that are involved. Morphological observations on the transformed material, even for single crystals of beta phase in the conditions described above, show the difficulties involved in obtaining a single crystal of martensite, without additional complications related to coalescence of domains of the same variant. Consequently, the measured energy has, at least, contributions from the elastic energy of interactions between different variants. In addition, internal stresses can generate new martensitic phases which coexist in the same crystal [15]. Therefore, knowledge of the energy exchanged without additional contributions is needed, i.e. the energy changes related exclusively to the motion of the interface. To achieve this, measurement must be under conditions where both temperature and dissipation/absorption change simultaneously. These conditions affect the behaviour of a calorimeter leading, in general, to changes in the base-line of the calorimeter.

In this paper an experimental set-up is described which enables the study of different aspects of the martensitic transformation of CuZnAl shape memory alloys. The experimental system was designed to allow us to work within restricted temperature ranges and to perform partial cycles and a detailed study of the material when only small motions of the interface are involved, for the reasons discussed above. In addition, this study also has direct relevance to cases in which the alloy is used as a mechanical switching device, i.e. when small temperature changes lead to small interface displacements which are then used as a triggering mechanism. We have chosen to concentrate on the acoustic emission released, on changes in resistivity and, using optical microscopy, on the evolution of the surface morphology of the material. We have also added a calorimetric device derived from unconventional differential scanning calorimeters [1,16]. The temperature of the sample is chosen to be a periodic function of time such that the average temperature is well inside the transformation region and the amplitude is small compared to the width of that region. Therefore, the kinetics of the forward and reverse transformation during their intermediate stages, can be studied.

TEMPERATURE CONTROL

The design is based on a previous experimental system devised to study the transformation by optical microscopy alone. The sample is placed on a block of copper (see Fig. 1). The block is heated or cooled by several thermoelements by use of the Peltier effect. The temperature of the copper block is controlled by a computer, see below.

The temperature control is done by using the transfer function of the system, that is, the functional relation between the power or intensity applied to the thermoelements, $I(t)$, and the increment in the temperature of the copper block produced, $T(t)$: $T(t) = F[I(t')]$, $t_0 < t' < t$. Ideally, $T(t)$ refers to the temperature of the sample although, in practice, it refers to the temperature of the copper block at a point near the location of the sample. Given $T(t)$, one has to determine the required power input $I(t)$ by solving the functional relation between the input and this temperature $T(t)$. If the system behaves linearly, F is a linear functional. In this latter case,

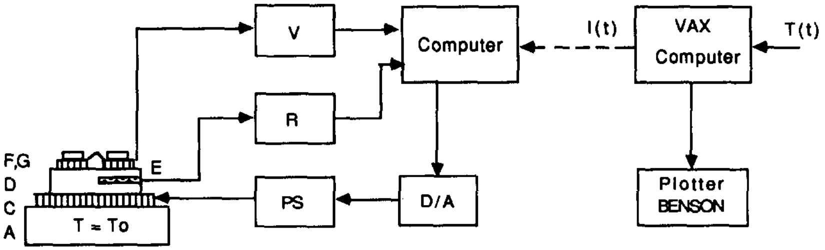

Fig. 1. Schematic diagram of the temperature-controlled device: A, heat sink, C, thermobattery MELCOR CP 1.0-127-06L; D, copper block; E, Pt = 100 platinum resistance; F, G, calorimetric thermobatteries MELCOR FC 0.6-66-05L; D/A, digital to analogic converter HP 59501B; PS, power supply HP 6284A; R, voltmeter HP 3478A; and V, voltmeter HP 3456A. The thermobatteries F and G can be suppressed and the sample attached directly on the copper block D. The broken line-arrow indicates that $I(t)$ is calculated from eqn. (3) with a VAX computer and then transferred to the personal computer which acts as an on-line controller.

the functional equation can be solved with a Fourier transform: $T(w) = TF(w)I(w)$. The Fourier transformation is defined as

$$G(w) = \int_{-\infty}^{\infty} G(t) \exp(-iwt)\, \mathrm{d}t \tag{1}$$

Because heat transport in a calorimetric device is a purely relaxational process, the response of the calorimetric device can be described by a transfer function TF (Laplace space) of the type

$$\mathrm{TF}(p) = \mathrm{TF}(p=0) \frac{\prod_i (1 + p\tau_i^\star)}{\prod_j (1 + p\tau_j)} \tag{2}$$

where $\mathrm{TF}(p = 0) = S$, is the sensitivity of the calorimeter, τ_i are the real poles of the system and $\tau_i^\star$ are sometimes referred to as the zeros of the system. The poles are obviously related to the characteristic time constants of the system and can be evaluated from the experimental response by standard techniques such as inverse filtering (the reader interested in the details of the technique is referred to refs. 17 and 18). It should be noted that the substitution of p by iaw leads to the Fourier transform of TF. Nevertheless, in practice, this transform is always computed using the F.F.T. algorithm.

Once $\mathrm{TF}(w)$ has been obtained, we can calculate the intensity which has to be supplied to the thermoelements, $I(t)$, to produce a given temperature program, $T(t)$, in the sample area, as

$$I(t) = \mathrm{F.F.T.}^{-1}\left[\frac{\mathrm{F.F.T.}(T(t))}{\mathrm{F.F.T.}(\mathrm{TF}(t))}\right] \tag{3}$$

where $\mathrm{TF}(t)$ is the experimental response to a Dirac input signal.

In order to smooth high frequency noise, a rectangular window is applied before performing the inverse Fourier transform. The resulting Gibbs phenomenon must also be smoothed.

These standard procedures are insufficient to achieve the resolution that we have discussed above. We are concerned here with very low frequencies (< 0.01 Hz). As a consequence, there are substantial changes in room temperature during the course of the experiment which requires some on-line corrections. We use feedback techniques to compensate for this secular change in the temperature (see Fig. 2). The correction which will be required depends strongly on the mass of the copper block and the complexity of the experimental device inside the working area (see Table 1). For instance, system A, which is the simplest, allows a cyclic temperature program of 2 K amplitude with periods of 200 s. System B allows a program of 50 K but requires periods of 1500 s. It should be noted that the amplitude of the temperature profile and the time constants of the calorimeter play an important role in the evaluation of the minimum period that can be used for a given resolution.

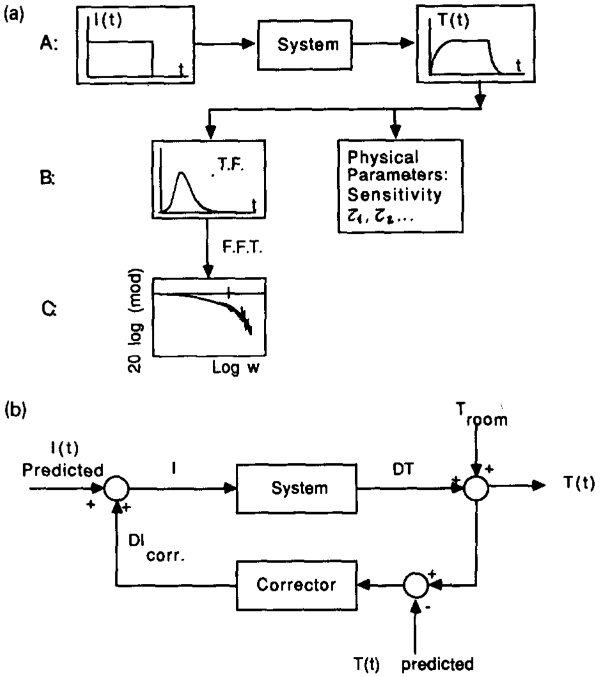

Fig. 2. (a) Scheme of the identification process: A, experimental measurement of the system response to a Heaviside input; B, calculation of the transfer function and determination of the sensitivity and time constants; and C, determination of the cut-off frequency. (b) Block diagram of the temperature control.

Table 2 shows the results of a test in which the measured temperature for homologous points of a periodic thermal cycling are compared. System C corresponds to the system labelled C in Table 1. The amplitude of the temperature program (see Fig. 3) is 0.130 Ω (from 23.290 to 23.628 °C). The

TABLE 1

First time constant for different kinds of working space; the mass of the copper block is included for each case

	Set-up [a]			
	A	B	C	D
m (g)	25	24	48	185
τ_1 (s)	65	74	135	225

[a] A: System used for optical microscopy observations. Parts F and G in Fig. 1 are not present.
B: System developed for calorimetric measurements, as shown in Fig. 1.
C: System similar to A but a stressing device made of copper is added above the copper block D.
D: System of the same kind as C.

TABLE 2

Acquired temperature expressed as resistance of the Pt-100 for homologous points of a periodic thermal cycle: *N* is the number of the cycle from which the data has been taken; the values in parentheses are explained in the text

N	System C			System B		
	1	2	17	1	2	5
a	109.201	109.200	109.200	118.300	118.300	118.301
				(117.615)	(117.629)	(117.639)
b	109.130	109.129	109.130	113.779	113.780	113.779
				(113.819)	(113.829)	113.842)
c	109.069	109.070	109.070	109.301	109.301	109.300
				(109.403)	(109.413)	(109.424)

a, Values at the maximum temperature.
b, Values half-way between the highest and lowest temperature.
c, Values at the lower limit.

period is 412 s, the slope is 7 mK s^{-1} and the temperature is kept constant at each extreme for 70 s. System B corresponds to the system B described in Table 1. The data shown are taken from a sinusoidal cycling between 23.886 and 47.149 °C with a period of 1500 s. The values in brackets were obtained with a second Pt-100 put above the calorimetric thermobatteries (this is the position where the sample will lie in the calorimetric runs). Some secular evolution is observed.

The results show that, from cycle to cycle, the reproducibility is better than 0.01 K for periodic temperature profiles. If the temperature of the sample were to be kept constant, the resolution is better than 0.003 K. These values lie near the limit of resolution of the resistance used (0.001 Ω).

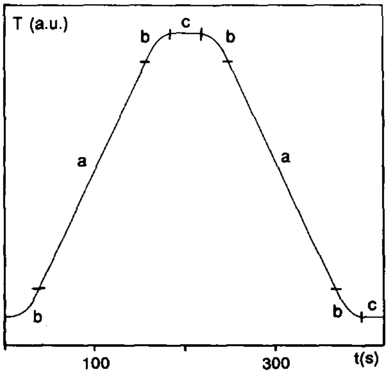

Fig. 3. A periodic temperature evolution such as those used in the experiments; three regions can be distinguished: a, linear evolution of the temperature at a given rate dT/dt; b, linking by two exponential terms; and c, constant temperature domains.

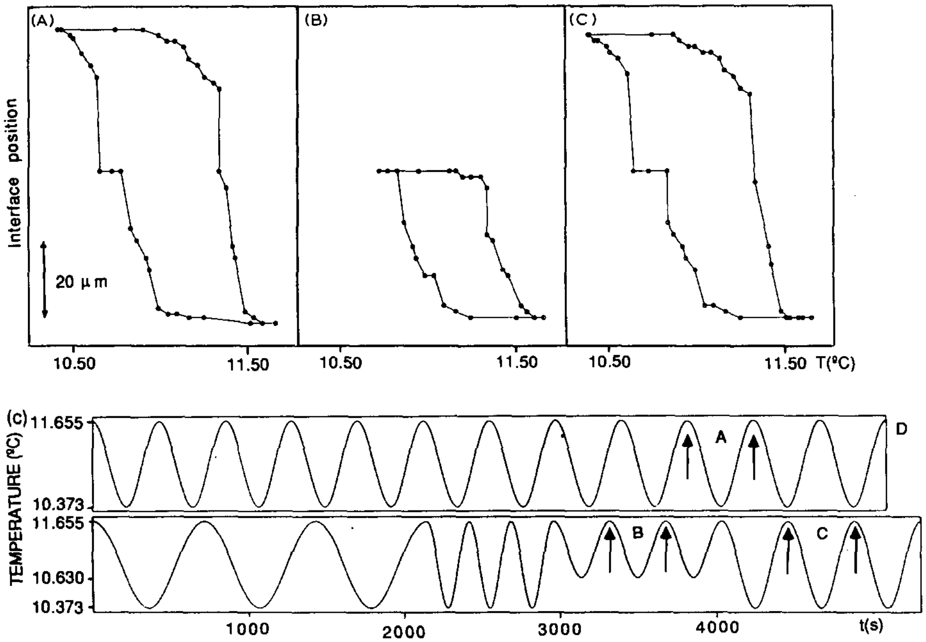

Fig. 4. Hysteresis cycles in interface position versus temperature coordinates (A, B and C) and continuous cycling sequence temperature versus time (D). The arrows point to the cycles to which the hysteresis plots belong. The dT/dt slope in A–C is the same and equal to 8.55 mK s^{-1}.

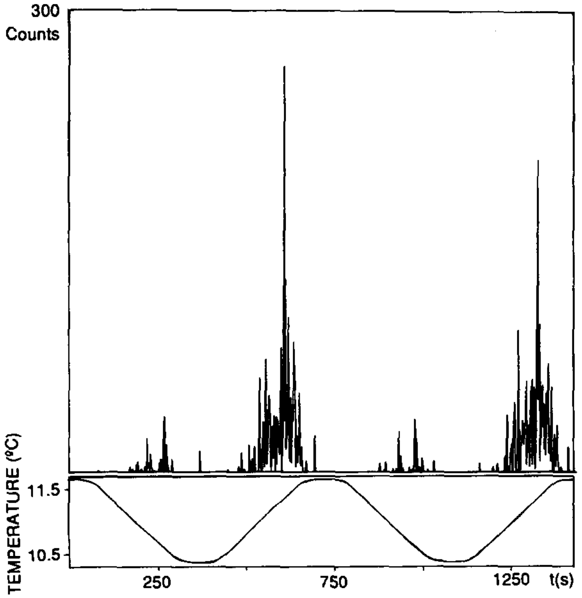

Fig. 5. Ring-down counting vs. time (top) and temperature vs. time (bottom) (cycles 13 and 14 in Table 3).

TABLE 3

Ring-down counting for several cycles (see Fig. 4D) versus temperature span and temperature rate; $A = 8.55$ mK s^{-1}, $B = 5.13$ mK s^{-1}, $C = 14.66$ mK s^{-1}; $a = 1.283$ K; $b = 1.026$ K

dT/dt	A	A	A	A	B	B	C	C	A	A	A	A	A
ΔT	a	a	a	a	a	a	a	a	b	b	a	a	a
Cycle number	5	6	8	10	13	14	16	17	19	20	22	23	24
Cooling	216	221	186	203	198	201	224	187	71	61	191	233	167
Heating	1665	1618	2053	1788	2084	2110	1713	1721	882	769	1530	1498	1495

Figures 4A–4C show the optical observations of the hysteresis cycle. We have measured the spontaneous growth and shrinkage of a martensite plate induced by a periodic temperature profile in the copper block (Fig. 4D). The hysteresis cycle is obtained by plotting the position of the interface (which is equivalent to the quantity of martensite present in the sample) versus temperature. Observations show how the hysteresis cycle is temperature controlled. Figure 5 and Table 3 show the measurement of the acoustic emission released (ring-down counting) for cycles in the same sequence of measurements. The standard deviation of the A.E. counting temperature rate $\Delta N/\Delta T$ is 14%.

RESISTANCE MEASUREMENTS

A precise determination of the electrical resistance of the sample can be used to determine the dynamical evolution of a single domain of martensite as it depends on the fraction of the sample that has transformed. Previous measurements of the resistivity for shape memory alloys do not have enough resolution to detect the elementary processes previously discussed in which we are interested [19]. Furthermore, coupled observations involving techniques of different resolutions (e.g. resistance measurements and acoustic emission detection) give rise to ambiguous interpretations [20].

We measure resistance changes during the martensitic transformation with the four points method. The resistance of a standard sample (length 22 mm, width 2 mm, thickness 0.3 mm) is about 1 mΩ. The changes in the resistance associated with the transformation are near 10%. The intensity of the current applied is 50 mA which leads to an energy dissipation near 53 μW. We use this intensity because it enables us to simultaneously obtain calorimetric information.

The voltages measured lie near 50 μV. In order to achieve a resolution better than 0.1%, we have introduced additional filtering on the signal. One way to reduce the effect of noise on the signal is to filter it by, say, reducing the bandwidth. One effective method of reducing the bandwidth without requiring too many adjustable components is the phase sensitive detection method (PSD), as applied to the detection of amplitudes [21]. In order to measure the amplitude of a signal, E_s, an additional modulation is added

$$e_s = E_s \sin(w * t + \Psi) \tag{4}$$

From the source of the modulation or from some other external source, one introduces a reference signal with a frequency w

$$v_r = V_r \cos(w * t) \tag{5}$$

In order to detect the original signal, assuming this is an electrical signal, an electronic circuit forms the product $e_s * v_r$. Then this product is low-pass filtered (for instance with an RC circuit). This procedure eliminates all the frequency components w' where $(w' - w)$ is not within a certain bandwidth. Then, very small frequencies in the low-pass filter can give a very narrow bandwidth system. The output of the system will be related to the input through $E_s\ V_r(\sin \Psi)/2$ [21].

However, if one tries to use a computer and an acquisition board to collect the data and then multiply and average it numerically, the situation is slightly different as the data set is now discretized. The most important difference with the analog case is that the digital device is not able to remove frequency components such that $w'' \geq \Pi/\Delta t'$, where $\Delta t'$ is the discrete sampling time interval. This drawback can be overcome by an analog low-pass filter before the acquisition board if w'' is far enough from the frequency of the reference w (i.e. one needs a large number of points per cycle of the reference frequency)

To use the lock-in technique, one must be sure that no DC components are present. In the case of analog systems, a capacitance or an AC/DC transformer coupling is enough. In digital systems, however, the problems from electrical insulation (ground loops, live-neutral connections, etc.) requires direct union and numerical operation to remove the offset. In fact, differences between low and earth levels in the instrumentation, in the interface board and in the computer must be reduced as well. The frequency of the AC generator must be chosen in such a way that the number of points sampled per period of the reference frequency be adequate (more than ten). We have chosen twenty sampled points per period as a compromise among the acquisition delay between consecutive tension and intensity data points, number of acquired data points (total acquisition time per measured resistance point) and number of periods of the reference signal needed to obtain significative measurements. As we need a number of periods high enough, we have used one hundred to two hundred periods in our case. The final resolution and reproducibility of the measurement will depend on the amplifiers' performances, the resolution in the data acquisition board and on the number of data points sampled.

A similar procedure following the same basic principle but that improves the resolution at low frequencies involves the use of square wave inputs. With this method the drift in the offset of the amplifiers is smoothed as it cancels over every period of the reference signal. However, and as a consequence of having modified the lock-in analyser principle, the low frequency noise is eliminated at the expense of introducing some noise near the frequency of the interest. With this technique, values of tension and intensity are sampled, and high and low levels are distinguished by removing the data which correspond to the rise and fall of the reference signal. In our case, values which do not lie within 10% of the top and bottom mean values

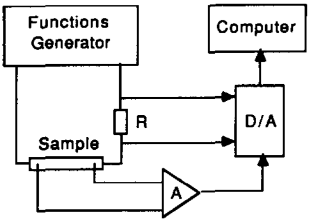

Fig. 6. Scheme of the configuration for the resistance measurements (temperature control not represented) consisting of a PC-computer with ADDA-14 board (analog to digital and digital to analog converter 14 bits), a Leader LB-102A function generator and a low noise amplifier.

are discarded. Next tension and intensity values are computed as differences between consecutive high and low mean values and averaged over the periods acquired. Finally, the resistance is calculated from the ratio between the tension and the intensity.

Fewer sampled points are required with this method because the maximum amplitude of the signal given by the generator is very accurate and stable. Furthermore, the use of given square wave signals provides two additional advantages: the power supplied is constant and only changes with the resistivity of the material (10% in the whole transformation); and deviations from linearity in the amplifiers in the working domain (from $-V$ to $+V$) are reduced, being simply the deviations around those extreme tensions.

The system which we have designed (see Fig. 6) allows us to measure the resistance while the computer controls the temperature of the sample. In

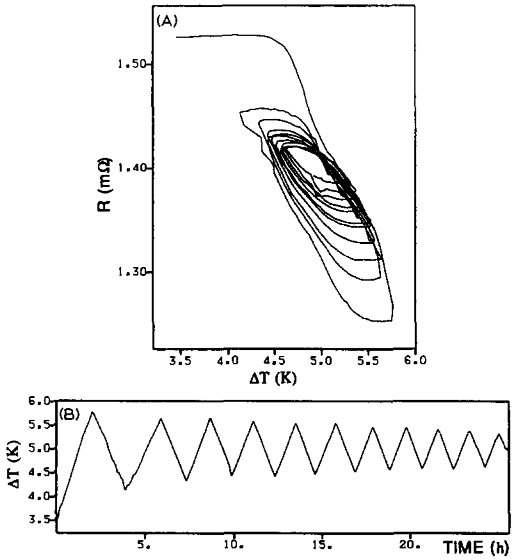

Fig. 7. Hysteresis evolution vs. temperature amplitude (mean temperature near 70 ° C): A, resistance vs. temperature; B, temperature vs. time.

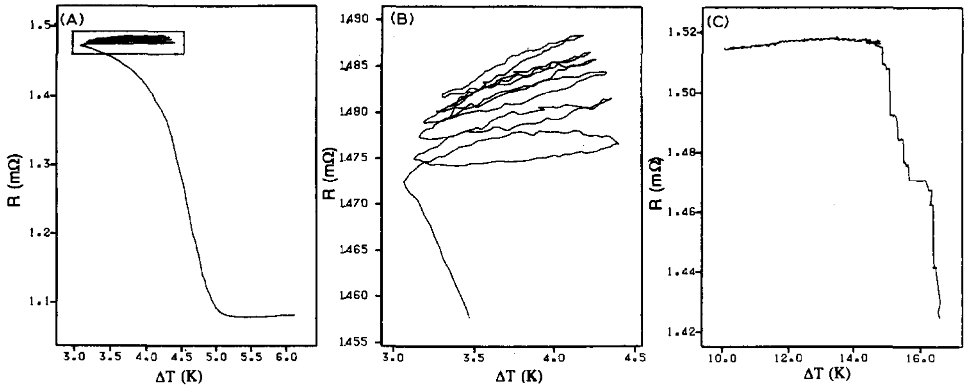

Fig. 8. Resistance vs. temperature: A, from β to martensite and local cycling; B, enlarged view of local cycling; and C, discontinuous steps in the local changes from martensite to β.

order to test the accuracy and reproducibility of the system, we have measured the resistance of a sample of electrolytic Cu of 2 mΩ. The results obtained show that the reproducibility in the measurement of the resistance with temperature is better than 0.04%. This result has been obtained over six cycles of 3.1 K amplitude at around 70 °C, for two days.

Figures 7A and 7B, and 8A–8C show the results from a sample of CuAlZn. Its composition (determined by EDAX) is Cu 76.9 wt.%, Al 5.3 wt.% and Zn 17.6 wt.%. The nominal M_s is 72 °C. Figure 7A shows the hysteresis cycle obtained from the measurement of the resistivity while the amplitude of the temperature domain (Fig. 7B) is reduced. Although the mean value of the temperature is still the same, the hysteresis cycle is smaller but there is a trend towards higher resistance when the martensite/parent phase is increased (martensite creep).

Figure 8B shows a fragment of a partial cycle (Fig. 8A) in which the growth in the amount of martensite is also shown. Figure 8C shows a limited range of the m–β transformation which allows one to see a discontinuous change in the resistance. This discontinuous behavior has also been observed with the acoustic emission bursts and in the calorimetric thermograms. This change is similar to those observed with AED or calorimetry, even from transformations supposed thermoelastic. We conclude that the discontinuous motion of the interface produces discontinuous changes in the resistivity. This is the first time that a discontinuity in the resistivity has been reported. Note that the amplitude of the discontinuity is larger than the accuracy.

DIFFERENTIAL SCANNING CALORIMETRY

This is a system based on the temperature program described in the first part. The calorimetric response is obtained by means of two plates of

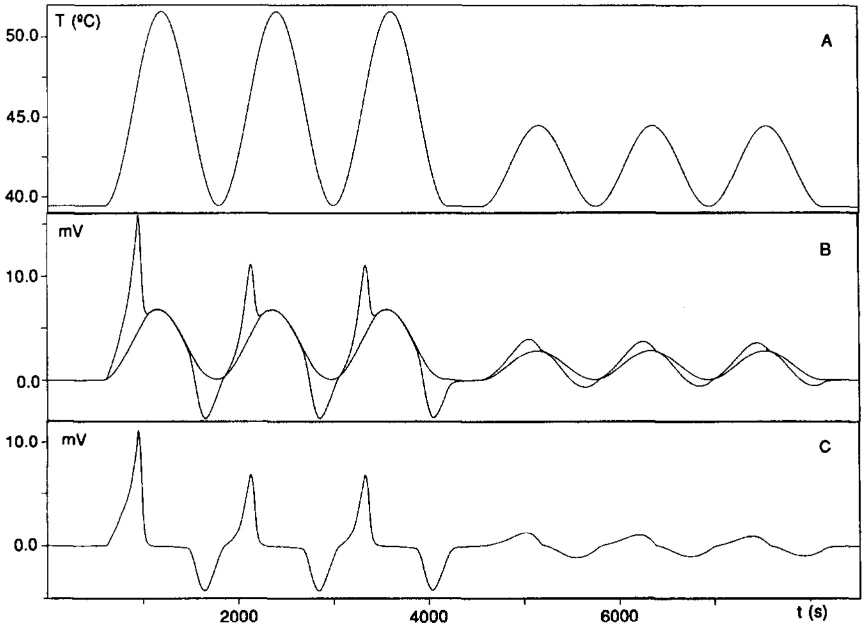

Fig. 9. A, temperature programming $T = T(t)$; B, thermogram and its base-line; C, thermogram when the base-line has been substracted.

MELCOR thermoelements of 1 cm^2 area, connected in differential (see Fig. 1). The temperature program affects the system in two different ways: due to the imperfect differentiability of the system, it gives a continuous change in the base-line, as can be seen in Fig. 9 in which an example of the temperature program and the resulting thermogram are presented; and the measured temperature is not identical to the temperature of the sample as it is measured at a different point.

TABLE 4

Amplitude ratio A and phase shift Ψ between the sinusoidal temperature programming and calorimetric response for different periods. The data corresponds to system B (see Table 1)

T (s)	ν (mHz)	A (mV K^{-1})	Ψ (rad) [a]
∞	0	0.64	
1820	0.55	0.65	+0.03
682	1.47	0.60	+0.09
512	1.95	0.56	+0.07
315	3.17	0.45	−0.10
256	3.91	0.40	−0.59
200	5.00	0.35	−1.10
150	6.67	0.41	−1.67
110	9.09	0.56	−2.00

[a] A positive Ψ indicates that the calorimetric signal reaches the maximum and minimum values before the temperature.

TABLE 5

Damping and phase shift between the temperature in the position of the sample and the controlled one, results obtained using system B (see Table 1)

T (s)	ν (mHz)	A (K K^{-1})	Ψ (rad)
682	1.47	0.95	0.20
256	3.91	0.85	0.49
110	9.09	0.63	0.92

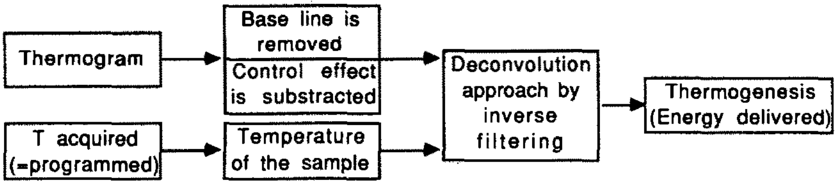

Fig. 10. Flow diagram from the experimental data to the final energetic measurement.

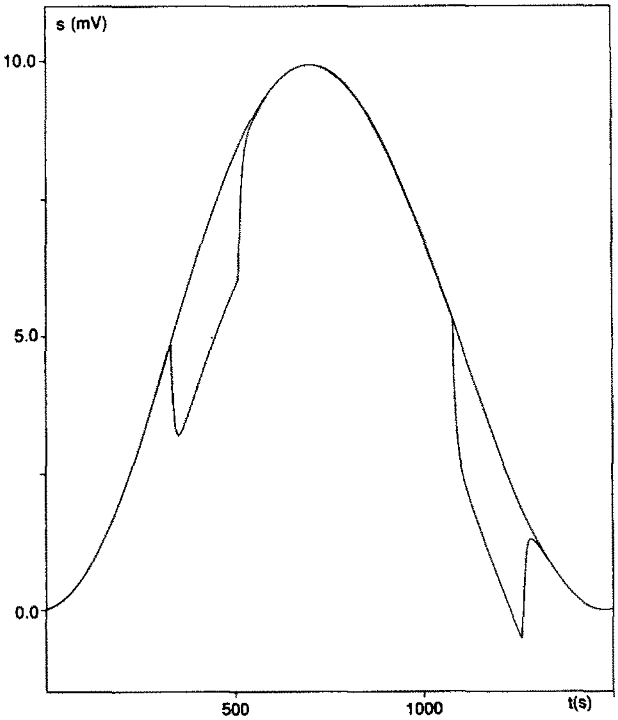

Fig. 11. Thermogram and its base-line correction (Joule effect studies) (see Table 7).

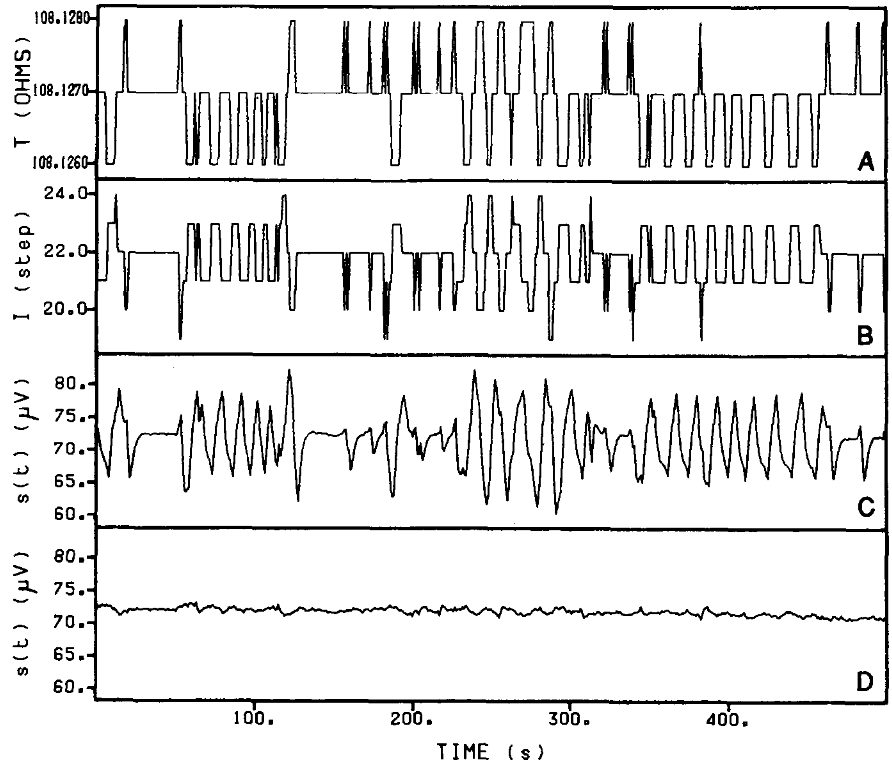

Fig. 12. Example of how the effect of the temperature control on the thermogram can be removed: A, temperature vs. time (temperature fluctuations near ±0.003 K); B, pattern of the intensity applied; C, thermogram acquired; and D, thermogram after the correction of the control effect.

Table 4 shows the amplitude ratio and the phase shift between the intended value of the temperature and the base-line. In Table 5, the same quantities are given but now referred to the programmed temperature and to a temperature measured exactly at the position at which the sample will be placed. In this case, the values were obtained using a Pt-100 platinum resistance sealed in glass and placed inside a 1.82 g sample. Therefore, smaller masses provide more reproducible temperature profiles.

The procedure to convert the calorimetric output to magnitudes adequate for the study of the transformation is summarized in Fig. 10. An example of the output and the base-line (obtained from zones without transformation) has been drawn in Fig. 11. We take into account the fact that there is a slightly variable phase shift between the temperature program and the base-line in the output obtained. This arises from the dependence of the sensitivity of the thermoelements on temperature and from the temperature program itself (see remark 1). In particular, the fluctuations in intensity one needs to ensure the desired values of $T(t)$ will induce fluctuations in the

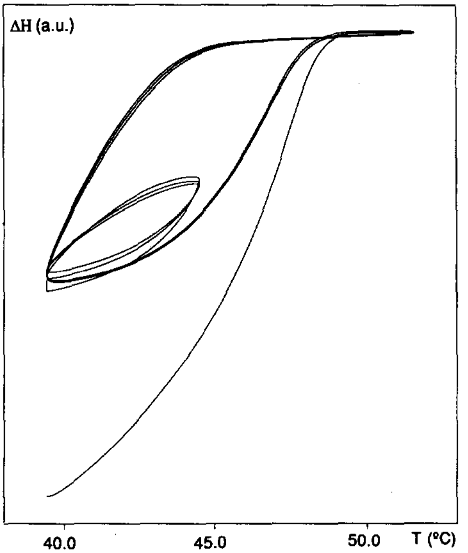

Fig. 13. Calorimetric hysteresis cycle plotted as the accumulated enthalpy vs. temperature, corresponding to the thermogram shown in Fig. 9.

output (see Fig. 12). This effect can be removed by subtracting the result of the convolution of this intensity fluctuation by using the initial calibration. After all these corrections have been taken into account, the uncertainty in the base-line is estimated to be ±1 μV which corresponds to an amount of heat released in the sample area of around 3 μW. This is one order of magnitude better than the resolution of standard systems.

The energy released during the transformation is determined from the output by means of a previous calibration. In the system described in this work, (see remark 2) the sensitivity of the device can be empirically approximated by

$$S(T)(\mathrm{mV/W}) = \frac{B1 * T + B0}{A2 * T^2 + A1 * T + A0} \tag{6}$$

TABLE 6

Enthalpies obtained (J) for a sequence of transformation $\beta \rightarrow$ m and m $\rightarrow \beta$. The sample has a composition 67.2% Cu, 5.1% Al, 27.7% Zn and a mass of 0.23 g

$\beta \rightarrow$ m	m $\rightarrow \beta$
−1.381	1.580
−1.366	1.520
−1.383	1.506
−1.370	1.530
−1.374	1.514
−1.389	1.536

with $B0 = 315.352$, $B1 = 9.52296$, $A0 = 1.00000$, $A1 = 0.0212936$ and $A2 = 3.52584\,\mathrm{E} - 5$. T is the temperature in degrees Celsius ($-50\,°\mathrm{C} < T < 80\,°\mathrm{C}$).

The enthalpy changes versus the temperature of the sample also yield the hysteresis cycle (see Fig. 13). The integral of $\mathrm{d}Q/T$, which is approximately equal to the change in the entropy of the transformation, can also be calculated. In Table 6, the values of the enthalpy changes for consecutive cycles of a sample of CuAlZn are presented. The uncertainty associated with the base-line fluctuations (± 1 μV) is, for this measurement, about 6 mJ. In addition, the error bars in the energy measurements have been analysed (see remark 2) and estimated to be around 1.5%. In our measurements, reproducibility is higher.

CONCLUSIONS

We have a temperature-controlled thermal analysis set-up with a resolution of 0.001 Ω (equivalent to 0.003 K), a reproducibility better than 0.01 K and a stability of ±0.003 K. From harmonic analysis, different profiles for the temperature evolution can be obtained.

The coupling of acoustic emission and optical microscopy reveals an intrinsic hysteresis, an intrinsic thermoelasticity (M_s and A_s function of the position) and a contribution of the surface effects (pinnings) to the hysteresis width and to the acoustic emission.

Resistance measurements with a resolution better than 0.1% over values of 1 mΩ are possible. Discontinuous changes in the resistance of a sample when transforming has been measured and related to the discontinuous growth of the martensite.

A calorimetric device controlled by a sophisticated temperature program is available. It can determine the energetic dissipations during partial or global cycles. The uncertainty on the base-line lies near ±1 μV or ±3 μW. Measurements with a reproducibility and accuracy better than 2% have been achieved.

REMARK 1

We have used two types of approximation in order to determine the base-line.

(a) If only restricted temperature ranges are considered, the base-line can be obtained with an identical temperature profile but above A_f or below M_s, where the material is in one phase (beta or martensite). This gives a good approximation to the base-line which would have been obtained inside the transformation domain.

(b) If the temperature range explored is large, non-linear effects become important. We have observed that phase shifts are slightly different for the maxima and the minima of the calorimetric output. Nevertheless, a linear

TABLE 7

Comparison between the energy delivered by Joule effect E_d and that calculated from the acquired thermogram E_c. The corresponding thermograms are similar to those shown in Fig. 11: sinusoidal temperature programming with a period of 1500 s between 25.95 and 46.65 ° C

Heating/cooling	H	C	H	C
E_d (J)	1.229	1.240	1.227	1.229
E_c (J)	1.202	1.234	1.218	1.219

correction for this phase shift seems to be sufficient to yield an acceptable reproducibility.

REMARK 2

The analysis of the accuracy of the technique used to measure energy changes has been done using a given temperature program and delivering power by means of resistance in the sample area. Table 7 shows the results obtained. The uncertainty in this measurement is estimated to be around 1.5%

ACKNOWLEDGEMENTS

Financial support from CAICYT (PPI 86-0079) and EURAM (0803/3 MA-1E-00120-C(GDF)) are gratefully acknowledged. Dr. R. Rapacioli, Dr. J.M. Guilemany and Dr. J. van Humbeeck are acknowledged for kindly providing the samples used in this work. Dr. F. Hierro is acknowledged for his aid in the determination of the samples composition by EDAX/SEM. Drs. C. Picornell and C. Segui are acknowledged for their aid in the acoustic emission studies. Dr. J. Viñals is gratefully acknowledged for his critical reading of the paper.

REFERENCES

1 H. Tachoire, J.L. Macqueron and V. Torra, in M.A.V. Ribeiro da Silva (Ed.), Thermochemistry and Its Applications to Chemical and Biochemical Systems, 1984, D. Reidel, pp. 77–126.
2 H. Tachoire, J.L. Macqueron and V. Torra, Thermochim. Acta, 105 (1986) 333.
3 C. Picornell, C. Seguí, V. Torra, C. Auguet, Ll. Mañosa, E. Cesari and R. Rapacioli, Thermochim. Acta, 106 (1986) 209.
4 R. Rapacioli, E. Cesari, C. Auguet and Ll. Mañosa, Rev. Metall. (Paris), 84(9) (1987) 69.
5 C. Picornell, C. Seguí, V. Torra, F.C. Lovey and R. Rapacioli, Thermochim. Acta, 113 (1987) 171.

6 C. Seguí, Thesis, Dep. Física, Universitat Illes Balears, Spain, 1987
7 C. Picornell, Thesis, Dep. Física, Universitat Illes Balears, Spain, 1987.
8 F.C. Lovey, E. Cesari, V. Torra and J.M. Guilemany, Mater. Lett., 5(4) (1987) 159.
9 F.C. Lovey, J. Ortin and V. Torra, Phys. Lett. A, 121(7) (1987) 352.
10 A. Amengual, F. Garcias, F. Marco, C. Segui and V. Torra, Acta Metall., 36(8) (1988) 2329.
11 A. Amengual, F.C. Lovey and V. Torra, unpublished results, 1989.
12 F.C. Lovey, J. Phys. (Paris), Colloq., 43 (1982) C4-585.
13 Videomagnetic tapes F01-1986 and F01-1989, Department de Física, Universitat Illes Balears, Spain.
14 M. Alhers, Prog. Mater. Sci., 30 (1986) 135.
15 J.V. Humbeeck, D.V. Hulle, L. Delaey, J. Ortin, C. Seguí and V. Torra, Trans. Jpn. Inst. Met., 28(5) (1987) 383.
16 C. Picornell, C. Seguí, V. Torra, J. Hernaez and C. Lopez del Castillo, Thermochim. Acta, 91 (1985) 311.
17 J. Navarro, E. Rojas and V. Torra, Rev. Gen. Therm. Fr., 12 (1973) 1137.
18 E. Cesari, V. Torra, J.L. Macqueron, R. Prost, J.P.Dubes and H. Tachoire, Thermochim. Acta, 53 (1982) 1 and 17.
19 K.V.S. Prasad and C. Bansl, Phys. Status Solidi A: 98 (1986) 453.
20 N. Nakanishi, T. Shigematsu, M. Yasuska, H. Oshima and J. Miura, Proc. of the ICOMAT, Nara-Japan, The Japan Inst. of Metals, 1986, p. 210.
21 D.P. Blair and P.H. Sydenham, J. Phys. E, 8 (1975) 621.